tvst

Article

Variability of Retinal Vessel Tortuosity Measurements Using a Semiautomated Method Applied to Fundus Images in Subjects With Papilledema

Heather E. Moss[1,2], Jing Cao[3], Munam Wasi[1], Steven E. Feldon[4], and Mahnaz Shahidi[5,6]

[1] Department of Ophthalmology, Stanford University, Palo Alto, CA, USA
[2] Department of Neurology & Neurological Sciences, Stanford University, Palo Alto, CA, USA
[3] Department of Statistical Science, Southern Methodist University, Dallas, TX, USA
[4] Department of Ophthalmology, University of Rochester, Rochester, NY, USA
[5] Department of Ophthalmology, University of Southern California, Los Angeles, CA, USA
[6] Department of Biomedical Engineering, University of Southern California, Los Angeles, CA, USA

Correspondence: Heather E. Moss, Byers Eye Institute at Stanford, 2370 Watson Court, Stanford University, Palo Alto, CA 94303, USA.
e-mail: hemoss@stanford.edu

Received: June 13, 2021
Accepted: November 28, 2021
Published: December 30, 2021

Keywords: papilledema; retinal vessels; tortuosity

Citation: Moss HE, Cao J, Wasi M, Feldon SE, Shahidi M. Variability of retinal vessel tortuosity measurements using a semiautomated method applied to fundus images in subjects with papilledema. Transl Vis Sci Technol. 2021;10(14):32, https://doi.org/10.1167/tvst.10.14.32

Purpose: To develop methods to quantitatively measure retinal vessel tortuosity from fundus images acquired in subjects with papilledema and assess sources of variability in these measurements.

Methods: Digital fundus images from 30 eyes of subjects with untreated idiopathic intracranial hypertension and papilledema were analyzed. Retinal vein and artery tortuosities for three to four vessels of each type were measured in a region of interest 1.8 to 2.7 mm from the center of the optic nerve head. Measurements were averaged to generate a venous tortuosity index (VTI) and arterial tortuosity index (ATI) for each eye. One image of each eye was analyzed two times by the same rater. Two images of each eye, differing by focal depth, were analyzed by the same rater. Correlations between VTI and ATI for the same image and different images were calculated.

Results: Intrarater Pearson correlations (r) were 0.8 (95% confidence interval [CI], 0.59–0.9) and 0.90 (95% CI, 0.73–0.96) for VTI and ATI, respectively, with one outlier removed. Interimage r values were 0.72 (95% CI, 0.48–0.87) and 0.96 (95% CI, 0.89–0.99) for VTI and ATI, respectively, with one outlier removed. The intraclass correlation coefficients for agreement and consistency were similar, suggesting that the discrepancy between measurements was due to residual random error.

Conclusions: The finding of similar intrarater and interimage variability suggests that intrarater variability may be a more dominant source than physiology and image acquisition.

Translational Relevance: Standardizing rater procedures and averaging multiple measuring sessions are strategies to reduce variability and improve reliability of detecting retinal vessel tortuosity changes in images of eyes with papilledema.

Introduction

The detection of intracranial hypertension (IH) is relevant for diagnosis of primary (idiopathic) IH (IIH) and secondary causes of IH including brain tumors, and venous sinus thrombosis as well as to inform treatment of these vision threatening conditions. Papilledema, swelling of the optic nerves, is a well-established marker of IH, but development and resolution are delayed after worsening and improvement of IH, respectively.[1] Changes in retinal vessels are a promising marker of IH on the basis of clinical observations of tortuosity, venous engorgement, vascular attenuation, and loss of spontaneous venous pulsations in individuals with untreated IIH compared with normal individuals.[2,3] Retinal vasculature markers of intracranial pressure (ICP) treatment may be superior to ophthalmic structural and vision based markers of ICP because they are more sensitive to dynamic

changes in disease status,[4,5] compared with structural changes of the optic nerve head (ONH).[6] Furthermore, they are clinically attractive as a marker of IIH treatment because they can be visualized easily through the pupil and can be quantified with noninvasive imaging technologies with high spatial and temporal resolution.[3,7–10]

Retinal venule diameter has received the most attention as a marker of ICP. It decreases within 1 hour after ICP lowering by lumbar puncture with cerebrospinal fluid drainage in individuals with high ICP,[11] within 1 month after optic nerve sheath fenestration in individuals with IIH,[12] after long-term therapy for IIH,[13] and after 6 months of medical and behavioral intervention in IIH.[14] An increase in the retinal venule diameter has been reported in animals[4,5] and humans after an acute ICP increase.[15,16] Experimental behavior of tubes under pressure suggests that increased retinal venule pressures mediate the association between greater venule diameters and an increased ICP.[2] Further support is provided by correlation between ICP and retinal venous pressures measured with ophthalmodynanometry.[17]

Other retinal vascular changes associated with altered retinal vascular pressures, such as tortuosity,[2] have not been previously investigated in IIH or other states with ICP change. A challenge with any retina vessel measurements in high ICP states is a distortion of the vascular anatomy by ONH swelling (papilledema). This eliminates the optic nerve boundary as a reliable landmark in image analysis. Accordingly, the objective of this project was to customize semiautomated retinal vessel tortuosity software for application to fundus images with papilledema and to evaluate imaging- and rater-based sources of measurement variability.

Methods

Images

Digital fundus images from 30 eyes were selected randomly from those that completed baseline and 6-month visits in the Idiopathic Intracranial Hypertension Treatment Trial (IIHTT), a randomized controlled trial of medical therapy for treatment of IIH, the full details of which are available elsewhere (NCT01003639).[18] The research adhered to the tenets of the Declaration of Helsinki and was approved by the institutional review boards of each center. Informed consent was collected from all participants in this study after they were notified of the nature and potential outcomes and consequences of the study. The current study was conducted using data from the IIHTT. It did not collect any new data and data were provided in a de-identified manner such that the identity of subjects could not be determined directly or indirectly. Therefore, the current study was exempt from institutional review board review (45 CFR part 46 requirements) under 45 CFR 46.101(b)(4).

Images for the current study were selected from those taken as part of the IIHTT study protocol at the baseline visit, specifically, two stereo pairs of 30° or 35° images that were centered on the ONH: one pair was focused on the dome of the disc and the other at the base of the disc. These fundus images were obtained through pharmacologically dilated pupils of at least 6 mm in diameter. Image acquisition protocols, including color and magnification calibration, were standardized across sites and personalized based on best-corrected visual acuity refraction to generate a calibrated data set.[19]

Two baseline images (one from each stereo pair) for each selected eye were included. Related to IIHTT trial entry criteria, subjects were untreated and had papilledema at baseline. Thus, all images used in the current study had papilledema.

Tortuosity Measurement

Our methodology allows a semiautomated image analysis to measure the tortuosity of individual retinal vessels using a calibrated color fundus image centered on the optic disc as the input. Manual identification of the ONH center as well as of the vessel end points was required. Our methodology was implemented using customized software (MATLAB r2019b, MathWorks, Natick, MA) and reflects a combination and modification of retinal vessel segmentation and retinal vessel tortuosity analysis tools previously developed by our group.[13,20–22] We briefly summarize the approach, highlighting modifications made for the current application. First, color fundus images were scaled according to the camera used for imaging and refraction per IIHTT photography reading center protocols[19] and converted to grey scale. Second, an image was generated using a two-dimensional Hessian filter that segmented the major retinal vessels. After a review of the filtered image using default parameters, the rater could adjust parameters to ensure that the vessels of interest were captured by the filter. Third, based on rater selection of ONH center and image calibration factor, a peripapillary ring-shaped region of interest (ROI) was defined with inner and outer radii of 1.8 and 2.7 mm from the ONH center, respectively. This ROI was chosen to align with the analysis grid used by the IIHTT photography reading center. Our previous work has suggested that this distance is likely to be relatively free from distortion from ONH swelling.[13]

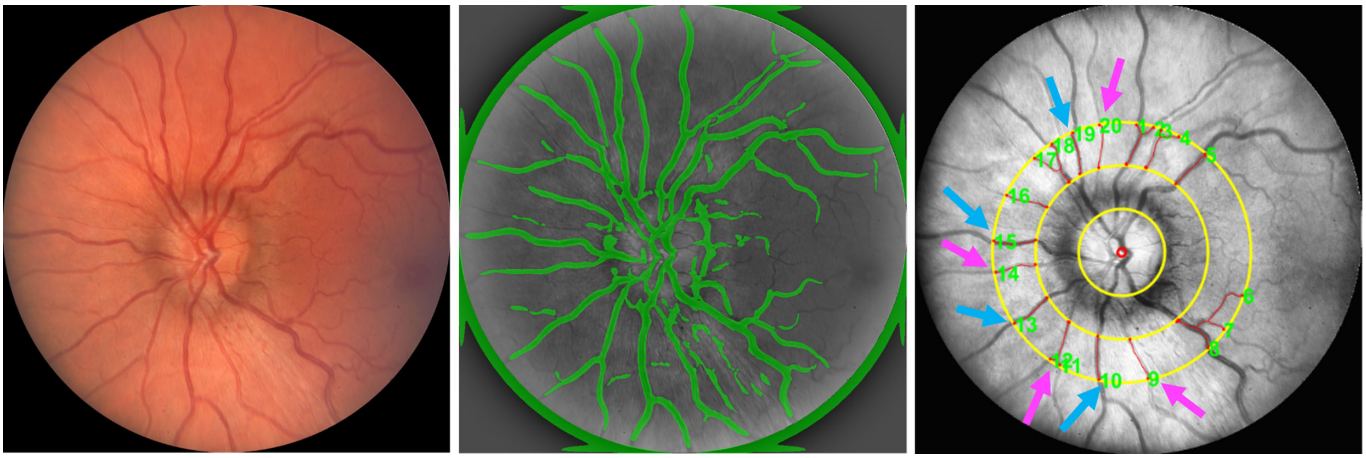

Figure 1. Measurement of retinal vessel tortuosity from fundus images centered on the ONH. Example of a color digital fundus image from a left eye (left). Segmented vessels are displayed in green overlaid on the gray scale image (center). ROI shown as a ring bounded by the two outer yellow circles, vessel centerlines shown in red, and selected arteries (purple arrow) and veins (blue arrow) used for measurements.

Fourth, using a binary image, the rater selected start and end points of each vessel in the ROI. The gray scale image was displayed simultaneously to guide vessel selection. Fifth, the vessel centerline was detected automatically and displayed to the rater for approval. Vessel tortuosity was calculated though use of geometric features to locate curves defined by inflection points (second derivative = 0) with a direction change in the vessel centerline's path. Curve magnitudes were quantified as the ratio of vessel segment length to straight line length between the curve end points to form the basis of the dimensionless vessel tortuosity index, as previously described.[20] This methodology generates a unitless vessel tortuosity index that is not impacted by rotation, translation, or magnification.

For each analysis, defined by image, rater, and session, a tortuosity index was calculated for three or four arterioles and three or four venules. The rater aimed for the selection of one of each vessel type in each quadrant. If this was not possible owing to branching or vessel overlap, alternative vessels were selected. Tortuosity indices of individual vessels of each type were averaged to generate venous tortuosity index (VTI) and arterial tortuosity index (ATI) for each analysis of each image. The image analysis protocol is outlined in Figure 1.

Intrarater Variability

For each eye, a single rater independently analyzed the same image on two occasions separated by more than 1 week.

Interimage Variability

The retinal vasculature is dynamic and a source of variability in images obtained on different occasions owing to changes in physiology. Another source of variability is image acquisition parameters, namely, image centering and focus. To assess the impact of these factors, the same rater independently analyzed one image from each stereo-pair for each eye. These images had been collected during the same IIHTT session with different focal depths.

Statistical Analysis

Intrarater variability as well as interimage variability were assessed for VTI and ATI using Pearson correlation, which calculates the strength of the linear relationship between different measurements. In addition, the intraclass correlation coefficient (ICC) was used to assess rater agreement, which can reflect both the degree of correlation and the agreement between measurements. ICC is calculated by mean squares obtained through analysis of variance models. Based on different analysis of variance models, the ICC can be used to measure absolute agreement and consistency among raters, where absolute agreement concerns both the systematic errors and of raters, whereas systematic differences between raters are irrelevant under consistency. Figure 2 plots three scenarios of rater reliability where Pearson correlation and two ICC measures—one for absolute agreement and one for consistency—are listed to demonstrate their differences. Analysis was performed using R (The R Foundation, Vienna, Austria).

Results

The VTI was successfully calculated for 27 eyes. The ATI was calculated for 18 eyes. For three eyes

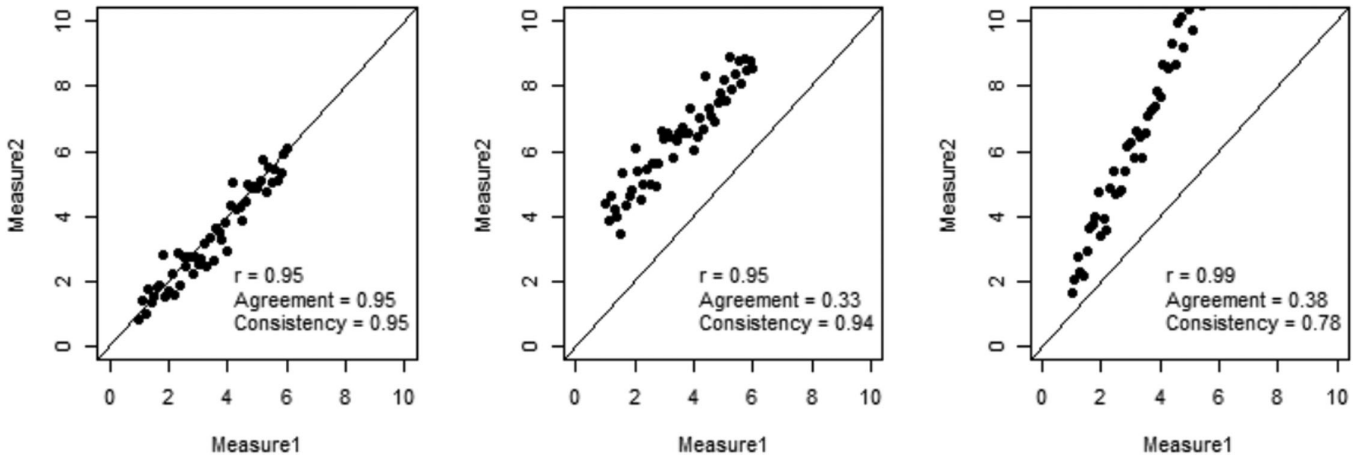

Figure 2. Three scenarios of rater reliability. In the left plot, the two measurements have a relationship of $Y = X + \varepsilon$, where ε is the random error. In the middle plot, the relationship is $Y = X + 3 + \varepsilon$. In the right plot, the relationship is $Y = 2X + \varepsilon$.

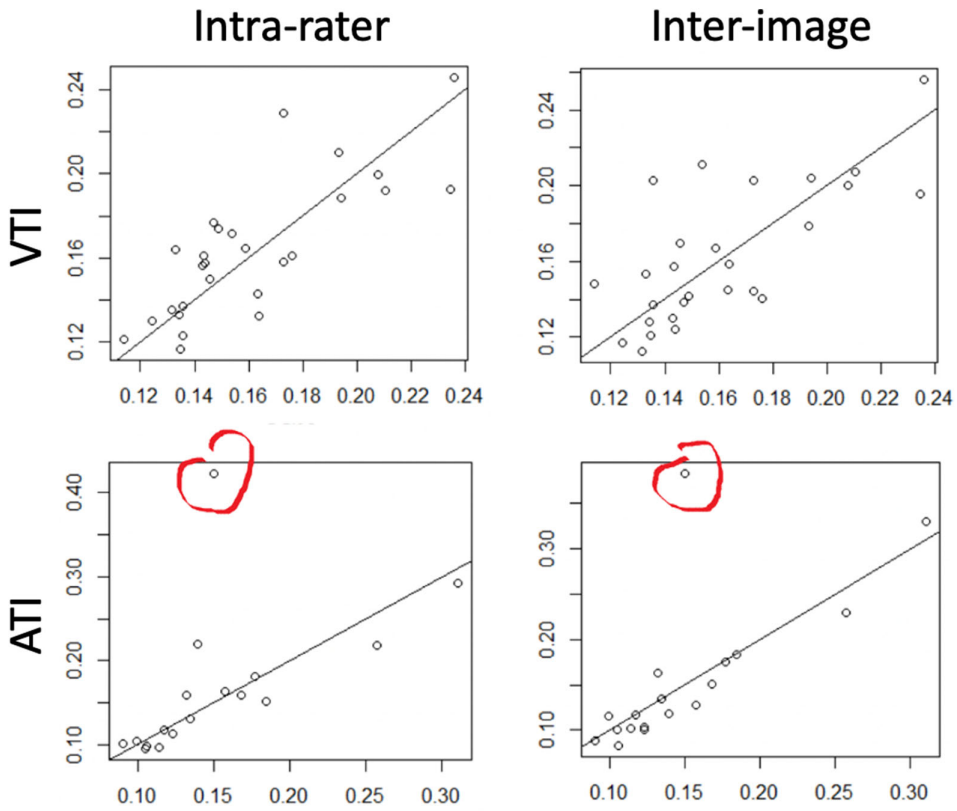

Figure 3. Intrarater and interimage comparisons for VTI and ATI. In each panel, the *x* axis and the *y* axis are VTI (top row) or ATI (bottom row) for analysis of an image. In the left column, the *x* and *y* values are for the same image analyzed by the same rater on two occasions. In the right column, the *x* and *y* values are for different images of the same eye analyzed by the same rater. A prominent outlier is shown in red.

neither VTI nor ATI were calculated. Indices could not be calculated in images for which fewer than three vessels of a single type were measured. The inability to measure the desired number of vessels was due to trouble identifying the type of vessel (eg, obscuration by the swollen optic nerve preventing tracking of vascular tree to verify arterial vs. venous origin) and trouble segmenting the vessels (eg, owing to branching and crossing in the ROI).

Intrarater and interimage comparisons for VTI and ATI are shown in Figure 3. For VTI, the Pearson r was 0.80 (95% confidence interval [CI], 0.59–0.90) for

Table. ICCs for VTI and ATI

	VTI ($n = 27$)	ATI ($n = 18$)	ATI Outlier Excluded ($n = 17$)
Intrarater			
ICC (agreement)	0.80 (0.61–0.90)	0.53 (0.10–0.80)	0.90 (0.75–0.96)
ICC (consistency)	0.80 (0.60–0.91)	0.53 (0.10–0.79)	0.89 (0.73–0.96)
Interimage			
ICC (agreement)	0.73 (0.49–0.87)	0.66 (0.29–0.86)	0.95 (0.88–0.98)
ICC (consistency)	0.73 (0.38–0.86)	0.65 (0.28–0.86)	0.96 (0.89–0.99)

Each table value is ICC (95% CI).

intrarater comparisons and 0.73 (95% CI 0.48–0.87) for interimage comparisons. For the ATI, the Pearson r was 0.57 (95% CI, 0.14–0.82) for the intrarater comparison and 0.70 (95% CI, 0.35–0.88) for the interimage comparison. There was a strong influence of a single outlier for ATI comparisons. On review of the images, this outlier was driven by different identification of the optic disc center by the rater on one image, which moved a branch point into the ROI and impacted the tortuosity index of a single vessel. Excluding this outlier, the Pearson r vales for the ATI were 0.90 (95% CI, 0.73–0.96) for intrarater and 0.96 (95% CI, 0.89–0.99) for interimage comparison. The ICC (95% CI) are shown in the Table.

Discussion

Retinal vessel tortuosity, essentially undulation or waviness of retinal vessels, is qualitatively detected by expert clinicians as a sign of retinopathy seen in association with hypertension and sickle cell disease among other conditions. Elevated pressure in tubes can cause tortuosity,[2] and thus it is a potential marker of ICP, which is associated with elevated retinal venous pressures.[17] To advance our understanding of retinal vessel changes in high ICP states, we developed a methodology for the assessment of retinal vessel tortuosity for application to fundus images with papilledema and assessed intrarater and intraimage variability. Although the sample size of 30 eyes may limit external validity, it was sufficient to evaluate the correlation between ratings and identify the sources of variability.

Tortuosity of retinal vessels occurs in some genetic conditions and in response to hypoxia, shear stress, and pressure and is a clinical marker of hypertension and hyperviscosity, among other conditions.[23] There has not been consensus on the mathematical definition of tortuosity. The simplest quantitative tortuosity measurement for a vessel segment is vessel length divided by the linear distance between the two end points, although many more complex approaches have been implemented. Our method mathematically detects inflection points based on a calculation of the angle of tangent lines for each point on a vessel's centerline and uses these values to derive segmental tortuosity ratios that are combined over the length of the vessel to generate a tortuosity index.[20] The measurement region is an important consideration when deriving vessel tortuosity from retinal images owing to variation in tortuosity in different parts of the retinal vascular tree. Often, the optic disc center and diameter form the basis of ROI identification.[24] Because this landmark is obscured when papilledema is present, we relied on image calibration on the basis of correction of refractive error to define the ROI.[19] A challenge in any retinal vessel assessment is bifurcations and overlapping vessels. We addressed this issue by selecting vessels without these features. An unexpected challenge was the difficulty of identifying retinal arterioles of suitable unobstructed length owing to papilledema associated vessel obscuration and this may limit application of our methodology to assessing arterial tortuosity in optic nerve images with high grade papilledema. An expanded field of view may be a strategy to mitigate this challenge.

In our study, there was a linear correlation for both intrarater and interimage comparisons. ICCs for rater agreement and rater consistency are close to each other, which implies that there is little systematic difference among the intrarater or interimage measurements. Thus, the discrepancies observed in the measurements are mainly due to random residual errors. One strategy to address these errors would be to average across analysis sessions. Although interimage and intrarater comparisons seemed to have similar variability, it is important to note that the interimage comparison is influenced by intrarater error, because the images were analyzed independently by the same rater. Given the similarity between the interimage and intrarater comparisons, we can conclude that the variability owing to retinal vasculature dynamics as a still image

and image focus variations are similar or less than that owing to the rater. Efforts to standardize rater procedures, particularly selection of the ONH center, which contributed to an outlier, will be important when applying this methodology to a data set for the purposes of understanding retinal vessel tortuosity associations with ICP and monitoring changes over time and after treatment.

Acknowledgments

Supported by the National Institutes of Health [Grants R21 EY031726, 1U10EY017281-01A1 (NORDIC), 1U10EY017387-01A1 (Data Coordination and Biostatistics Center), 3U10EY017281-01A1S1 (American Recovery and Reinvestment Act for NORDIC), 1U10EY017387-01A1S1 (Data Coordination and Biostatistics Center), 3U10EY017281-01A1S2 (supplements for NORDIC), P30 EY026877 and EY029220], Research to Prevent Blindness [unrestricted grants to the Departments of Ophthalmology at the University of Rochester, University of Southern California and Stanford University].

Disclosure: **H.E. Moss,** None; **J. Cao,** None; **M. Wasi,** None; **S.E. Feldon,** None; **M. Shahidi,** None

References

1. Hayreh MS, Hayreh SS. Optic disc edema in raised intracranial pressure. I. Evolution and resolution. *Arch Ophthalmol*. 1977;95:1237–1244.
2. Kylstra J, Wierzbicki T, Wolbarsht M, Landers M, Stefansson E. The relationship between retinal vessel tortuosity, diameter, and transmural pressure. *Graefes Arch Clin Exp Ophthalmol*. 1986;224:477–480.
3. Moret F, Poloschek CM, Lagrèze WA, Bach M. Visualization of fundus vessel pulsation using principal component analysis. *Invest Ophthalmol Vis Sci*. 2011;52:5457–5464.
4. Rios-Montenegro EN, Anderson DR, David NJ. Intracranial pressure and ocular hemodynamics. *Arch Ophthalmol*. 1973;89:52–58.
5. Ghate DA, Gulati V, Havens S, et al. Episcleral venous pressure and intraocular pressure as biomarkers for intracranial pressure changes. *Invest Ophthalmol Vis Sci*. 2017;58:4305–4305.
6. Hayreh MS, Hayreh SS. Optic disc edema in raised intracranial pressure. I. Evolution and resolution. *Arch Ophthalmol*. 1977;95:1237.
7. Patton N, Aslam T, MacGillivray T, Pattie A, Deary IJ, Dhillon B. Retinal vascular image analysis as a potential screening tool for cerebrovascular disease: a rationale based on homology between cerebral and retinal microvasculatures. *J Anat*. 2005;206:319–348.
8. De Jong F, Schrijvers E, Ikram M, et al. Retinal vascular caliber and risk of dementia The Rotterdam Study. *Neurology*. 2011;76:816–821.
9. Haan M, Espeland M, Klein B, et al. Cognitive function and retinal and ischemic brain changes The Women's Health Initiative. *Neurology*. 2012;78:942–949.
10. Hubbard LD, Brothers RJ, King WN, et al. Methods for evaluation of retinal microvascular abnormalities associated with hypertension/sclerosis in the Atherosclerosis Risk in Communities Study. *Ophthalmology*. 1999;106:2269–2280.
11. Moss HE, Vangipuram G, Shirazi Z, Shahidi M. Retinal vessel diameters change within 1 hour of intracranial pressure lowering. *Transl Vis Sci Technol*. 2018;7:6.
12. Lee SY, Shin DH, Spoor TC, Chaesik K, McCarty B, Kim D. Bilateral retinal venous caliber decrease following unilateral optic nerve sheath decompression. *Ophthalmic Surg*. 1995;26:25–28.
13. Moss HE, Treadwell G, Wanek J, DeLeon S, Shahidi M. Retinal vessel diameter assessment in papilledema by semi-automated analysis of SLO images: feasibility and reliability. *Invest Ophthalmol Vis Sci*. 2014;55:2049–2054.
14. Moss HE, Hollar RA, Fischer WS, Feldon SE. Retinal vessel diameter changes after 6 months of treatment in the Idiopathic Intracranial Hypertension Treatment Trial. *Br J Ophthalmol*. 2020;104:1430–1434.
15. Steffen H, Eifert B, Aschoff A, Kolling GH, V√∂lcker H. The diagnostic value of optic disc evaluation in acute elevated intracranial pressure. *Ophthalmology*. 1996;103:1229.
16. Entezari M, Azhari S, Ramezani A. Fundus findings in spontaneous subarachnoid hemorrhage and their correlation with neurologic characteristics. *Eur J Ophthalmol*. 2009;19:460–465.
17. Firsching R, Schutze M, Motschmann M, Behrens-Baumann W, Meyer-Schwickerath R. Non-invasive measurement of intracranial pressure. *Lancet*. 1998;351:523–524.
18. Wall M, Kupersmith MJ, Kieburtz KD, et al. The idiopathic intracranial hypertension treatment trial: clinical profile at baseline. *JAMA Neurol*. 2014;71:693–701.

19. Fischer WS, Wall M, McDermott MP, Kupersmith MJ, Feldon SE. Photographic reading center of the Idiopathic Intracranial Hypertension Treatment Trial (IIHTT): methods and baseline results. *Invest Ophthalmol Vis Sci*. 2015;56:3292–3303.
20. Khansari MM, O'Neill W, Lim J, Shahidi M. Method for quantitative assessment of retinal vessel tortuosity in optical coherence tomography angiography applied to sickle cell retinopathy. *Biomed Opt Express*. 2017;8:3796–3806.
21. Garvey SL, Khansari MM, Jiang X, Varma R, Shahidi M. Assessment of retinal vascular oxygenation and morphology at stages of diabetic retinopathy in African Americans. *BMC Ophthalmol*. 2020;20:295.
22. Khansari MM, Garvey SL, Farzad S, Shi Y, Shahidi M. Relationship between retinal vessel tortuosity and oxygenation in sickle cell retinopathy. *Int J Retina Vitreous*. 2019;5:47.
23. Vilela MA, Amaral CE, Ferreira MAT. Retinal vascular tortuosity: mechanisms and measurements. *Eur J Ophthalmol*. 2020;1120672120979907.
24. Kalitzeos AA, Lip GY, Heitmar R. Retinal vessel tortuosity measures and their applications. *Exp Eye Res*. 2013;106:40–46.